

Universality in multispecies traffic

Georg Anagnostopoulos^{*1} and Nikolas Geroliminis¹

¹*Urban Transport Systems Laboratory, School of Architecture, Civil and Environmental Engineering, EPFL, CH-1015, Lausanne, Switzerland*

January 7, 2025

Abstract

Understanding the nature of traffic heterogeneity is of major importance, given the widespread adoption of micromobility in cities. Based on massive field data and a nonequilibrium model, we demonstrate that heterogeneous, multispecies traffic is a member of an inherently nonequilibrium universality class associated with porous flows, namely directed percolation (DP) in one spatial dimension. Our central finding is that, macroscopically, multispecies traffic behaves like water percolating through a porous medium. This hypothesis remained unresolved for years mainly due to the incompatibility of equilibrium approaches with phenomena that are quite far from equilibrium and the limited resonance of complexity theory in the transportation literature. DP entails the existence of a nontrivial phase transition from a disordered subcritical phase to an ordered supercritical phase that depends on a temperature-like control parameter and is governed by a universal power-law. Our model explains the large scatter found in experimental data by taking into account the nonlinear, stochastic perturbations present in multispecies traffic configurations due to coupling of a predominantly lane-based host system with a layer of lane-free parasitic flows.

^{*}Correspondence and requests for materials should be addressed to G.A. (email: georgios.anagnostopoulos@epfl.ch).

Several years ago, it was conjectured that heterogeneous traffic behaves like a porous flow, “where smaller vehicles *percolate* to the front of the queue”¹, much like water infiltrating a bed of coffee grounds. Surprisingly, the authors of that early paper overlooked the *already established percolation theory*^{2,3}, leaving their conjecture unsubstantiated to this day. Understanding the nature of traffic heterogeneity is evidently of major relevance, particularly given the widespread adoption of *micromobility*⁴ in cities, where distinct populations of vehicles often share the infrastructure. An example of such a multispecies⁵ system (see Fig. 1a and Supplementary Movie 1) is thoroughly documented in the pNEUMA⁶ traffic dataset, which includes half a million trajectories spanning an expansive 1.3 km² area in the congested central business district of Athens, Greece.

Empirically motivated by the pNEUMA data and leveraging simulation techniques as a stepping stone, we show that multispecies traffic is a member of the *universality class* associated with porous flows, namely directed percolation (DP)³ in one spatial dimension (1D). DP universality is intimately linked to the idea of *self-organized criticality* (SOC)^{8,9}, which implies the existence of critical attractor points that are reached by the system spontaneously without meticulous tuning of control parameters. Physical systems of the same universality class may share the same critical properties, independent of the details of the problem formulation or mathematical model. Universality thus allows us to assert that, near the critical point, “the model describes the nature of a real system exactly”⁷, ensuring the model’s physical correctness. Conversely, a model that fails to exhibit the expected critical behavior can be safely dismissed.

SOC is simply absent in traffic models that rely on strong equilibrium assumptions, such as the Lighthill-Whitham-Richards (LWR)^{10,11} theory and its multispecies extensions^{1,12}, where the system is completely determined by the initial conditions. Even so-called *nonequilibrium*¹³ traffic models only add a relaxation term to the dynamics, whereas true nonequilibrium processes capable of criticality and phase-transitions are driven, noisy systems of *active matter*^{14–16}. In these systems, criticality emerges from the interplay between relaxation and stochastic driving terms⁷.

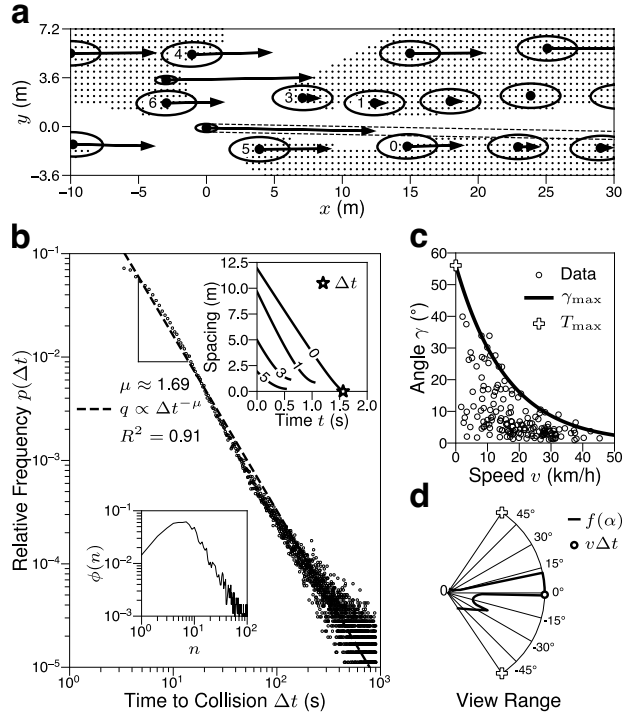


Figure 1: Empirical results from the pNEUMA data. **(a)** Snapshot of an actual urban arterial road with multispecies traffic. The different vehicle geometries are approximated as inscribed hard elliptical discs. Arrows indicate velocity vectors in m/s. Using the symmetric shadowcasting technique, we perform a visibility analysis in discrete space with a resolution of 45 cm, small enough to also detect microvehicles. **(b)** Upper inset: Assuming constant velocities, we compute the minimum time to collision Δt between the microvehicle at (0,0) and its visible, converging neighbors {0, 1, 3, 5}. Main panel: at the sample level (Supplementary Data 1), the histogram $p(\Delta t)$ has a power-law objective distribution $q \propto \Delta t^{-\mu}$. Lower inset: the same data yields a frequency distribution $\phi(n)$ of the bin counts n , which is also heavy-tailed⁷. **(c)** View range γ_{\max} is a function of vehicle speed, with data points showing actual maneuver events (Methods, Supplementary Data 2). The intercept is T_{\max} . **(d)** Interpretation of the same situation as in the first-panel, but from the agent’s spatiotemporal point of view, considering the dynamic porosity $f(\alpha)$.

The incompatibility of equilibrium theories with recent empirical evidence becomes apparent in the pNEUMA field experiment, where various types of scooters and motorcycles—hereinafter referred to as microvehicles⁴—appear with a notable frequency of up to 30%. Predicting the erratic dynamics of these microvehicles lies beyond the scope of the LWR model, which is widely regarded as the foundation of traffic flow theory. In the absence of a reliable alternative, transportation researchers tend to disregard the micromobility aspect of pNEUMA by excluding all microvehicle data. However, this common practice is methodologically flawed. To understand why, we must introduce the idea of *anticipation*.

Anticipatory models^{17–20} involve a spatiotemporal metric of *time to collision* Δt that is defined as the anticipated time at which pairs of non-omniscient, visually obstructed agents, approximated here as inscribed, hard elliptical discs²¹, will collide if they keep converging at their current velocities (Fig. 1a-b). Δt is particularly useful because theoretical equilibrium conditions are attained when $\Delta t \rightarrow \infty$. However, Fig. 1b shows that, even if we only plot car data, Δt has a textbook *power-law objective distribution*⁷ $q \propto \Delta t^{-\mu}$ that is statistically sound²². To the best of our knowledge, this power-law is reported here for the first time, indicating that equilibrium conditions occur as rare events drawn from a heavy-tailed distribution. It also empirically verifies that multispecies traffic is an intrinsically far-from-equilibrium system.

Before diving into the results, a brief note on the overall methodology is provided to guide the reader. Instead of developing a theory-based model, simulating it, and then conducting a controlled experiment in the real world to validate a preconceived theory, we do the opposite: we propose a theory-agnostic, *heuristic*²³ model calibrated on field data from an uncontrolled experiment, and then identify a theory that explains our results. This approach works for two reasons: Firstly, if the simulation fits the real data as well as the theoretical expectation, then, by causal association, the identified theory should offer a satisfactory explanation for the underlying data-generating natural process. Secondly, some variables might not be readily observable in reality, but are accessible to the analyst in a simulated environment.

Results

In line with our empirical findings, we propose in this communication an intrinsically nonequilibrium model for multispecies traffic, which consists of two pillars: a steering and a velocity module. By coupling two simple nonlinearities in the respective modules, we obtain a novel mechanism for 1D directed percolation in continuous space and time. This mechanism can also be interpreted from a statistical point of view in terms of a *sample space reducing* (SSR)^{24,25} process.

Using custom simulation software, we model a straight road with two lanes, each of standard width $W = 3.6$ m and length $L = 90$ m, with periodic boundary conditions. For the initial conditions, we employ Poisson disk sampling²⁶, a fast dart-throwing algorithm, to generate feasible, randomized spatial distributions of microvehicles for any given linear car density (Supplementary Fig. 1). Samples are then drawn *without replacement* from this feasible set. Our results are based on ensemble averages from 256 independent simulation runs. Each simulation begins with all agents at rest and concludes after a duration of $\delta t = 180$ s, with only the last $\delta t^* = 60$ s reported, as they are sufficiently far from the transient phase. In stark contrast to traditional equilibrium methods, we do not require an initial perturbation event, since the system is constantly driven far from equilibrium (see Supplementary Movie 2).

Steering with dynamic view range

Navigating an out-of-equilibrium crowd is a tough task that involves decision-making under uncertainty and incomplete information. In this situation, agents adapt their steering behavior by adjusting their field of view γ_{\max} (Fig. 1c-d) in a dynamic, nonlinear manner, based on their instantaneous speed v :

$$\log \gamma_{\max}(v) = bv + c, \quad (1)$$

where the parameters b and c are obtained by means of *quantile regression*²⁷ (see Supplementary Table 1). Equation (1) only provides a dynamic upper bound, while the actual angle $\gamma < \gamma_{\max}$ for each maneuver is the result of a stochastic process, as explained below.

From the angle γ_{\max} , we define a dynamic view range as the discrete choice set $\alpha \in \{\alpha^-, \alpha^+\}$, where α has a half-degree resolution in the reference frame of the vehicle, such that $\alpha^+ - \alpha^- = 2\gamma_{\max}$. Next, the time to collision at the *desired velocity* v_0 is calculated for each angle α , denoted $\Delta t(\alpha)$ in equation (2)¹⁸. Given a horizon distance d_{\max} that depends on the system size, we specify the distance to collision $f(\alpha)$:

$$f(\alpha) := \min\{d_{\max}, v_0 \Delta t(\alpha)\}, \quad (2)$$

which is always defined, even if Δt is not identified, and is a measure of *dynamic porosity*. Comparing the situation in Fig. 1a with its perception in Fig. 1d, we observe that $f(\alpha)$ can behave counterintuitively, contradicting the static¹ understanding of porosity. The objective of the dynamic porous heuristic is to probe for an optimal collision-free direction α^* that also minimizes the spatiotemporal detour $d(\alpha)$ from a target direction α_0 (square form used for efficiency):

$$d(\alpha)^2 = d_{\max}^2 + f(\alpha)^2 - 2d_{\max}f(\alpha)\cos(\alpha_0 - \alpha). \quad (3)$$

A *random choice* is made if multiple solutions for $\alpha^* = \operatorname{argmind}(\alpha)^2$ exist. In contrast to models of homogeneous crowds^{18,28}, where a_0 points to a fixed egress location (e.g., a gate), we propose a dynamic targeting mechanism. Because in multispecies traffic larger vehicles act as moving obstacles, microvehicles propagate towards the direction of least resistance or higher porosity. Defining $g := \max\{f(\alpha^-), f(\alpha^+)\}$, we aim to find α_0 , such that $f(\alpha)$ is maximized:

$$a_0 = \begin{cases} 0, & g = d_{\max} \\ \operatorname{argmax} f(\alpha), & g < d_{\max}. \end{cases} \quad (4)$$

If Δt is undefined at the limits of the view range, the agent maintains $\alpha_0 = 0$. Steering is then governed by the following ordinary differential equation (ODE):

$$\dot{\alpha} = \tau^{-1} [\alpha^* - \alpha], \quad (5)$$

where τ is a constant time-relaxation. For simplicity, we assume no lateral dynamics for cars in this model.

At this point it should be clear that a dynamic view range is equivalent to an SSR process in the sense that each decision results to a nonlinear adjustment of the sample space, much like rolling a shape-shifting die²⁴. The view range can also be understood as a measure of noise^{8,14} or a (directed) percolation^{2,3} probability.

Heterogeneous optimal velocity model

In this section we develop a novel optimal velocity (OV)²⁹ model that is *heterogeneous, stochastic and nonlinear*. An OV is a phenomenological mapping of the spacing s to an optimal velocity $V(s)$, where V must satisfy general conditions of continuity and monotonicity. We start by reviving a functional form for V that was first introduced as part of Newell's Nonlinear Model (NNM)^{30,31}. As Newell writes, “no motivation for this choice is proposed other than the claim that it has approximately the correct shape and is reasonably simple”. Although originally proposed for homogeneous car traffic, this nonlinearity predicts microvehicle dynamics surprisingly well (Fig. 2a).

The NNM has 3 shape parameters plus an explicit reaction time, which we substitute by an implicit speed adaptation time. The shape parameters are the jam spacing s_0 , the slope at the jam spacing $\lambda = V'(s_0)$ and a desired velocity v_0 . Accordingly, $V : s \mapsto V(s)$ has the following formal specification:

$$V(s) := \max\{0, v_0 - v_0 \exp[-\lambda v_0^{-1}(s - s_0)]\}. \quad (6)$$

Heterogeneity arises when each agent n receive their own response curve V_n . As a consequence, the 3 deterministic parameters are distributed and model calibration becomes a two-staged problem. Firstly, the parameters for each driver/rider are estimated by nonlinear least squares fits (Fig. 2a). Secondly, positive continuous distributions are estimated from the obtained populations of empirical parameters by standard maximum likelihood estimators, assuming independence (Supplementary Table 3-4). This is a reasonable assumption following from the fact that the chosen shape parameters are intended to capture completely different behavioral qualities and should be ideally uncorrelated.

Last but not least, temporal stochasticity is a key feature of nonequilibrium traffic. We assume that each V_n is imperfect and subject to perturbations from an error source ε_n modeled as an Ornstein-Uhlenbeck (OU) stochastic process, resulting in:

$$\begin{cases} \dot{\varepsilon}_n = -\tau^{-1}\varepsilon_n + a\xi_n, \\ \dot{v}_n = \tau_n^{-1}[w(V_n + \varepsilon_n) - v_n], \\ \dot{x}_n = v_n, \end{cases} \quad (7)$$

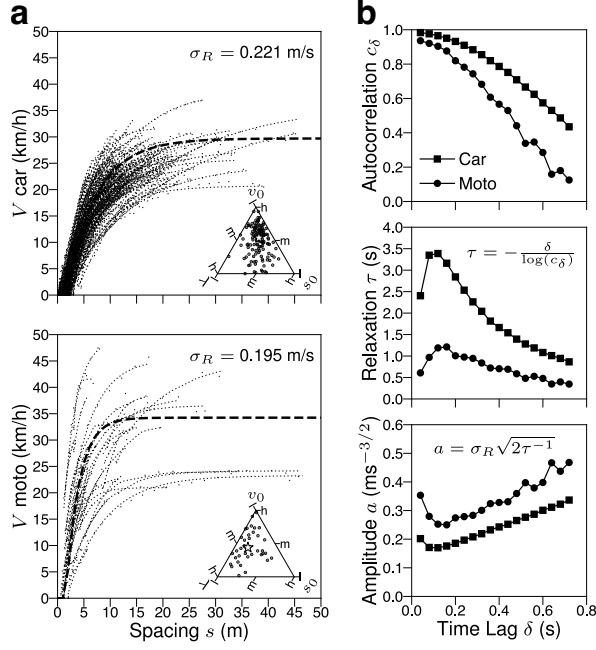


Figure 2: Model estimation considering distributed deterministic parameters and a stochastic process. **(a)** Speed-spacing responses fitted on pNEUMA data (Supplementary Data 3). Each curve corresponds to strictly 1 human subject, but each individual may engage in different dynamics. We consider in total 29208 driving observations corresponding to $C_{\text{car}} = 135$ curves, and 2976 riding observations corresponding to $C_{\text{moto}} = 38$ curves. The ratio $C_{\text{moto}}/(C_{\text{moto}} + C_{\text{car}})$ is representative of the split in the real data with 20-25% motorcycles. Ternary plots show the curves of each species as points in 3D parameter space using barycentric coordinates. **(b)** Model error is captured by a stochastic process. First, the autocorrelation functions c_δ^{car} and c_δ^{moto} of the residuals are calculated for several increasing time lags δ in steps of 0.04 s, that is identical to the time resolution of the dataset. We can then compute the noise relaxation time $\tau = -\delta / \log(c_\delta)$ and the noise amplitude $a = \sigma_R \sqrt{2\tau^{-1}}$, where σ_R is the standard deviation of the residuals from the nonlinear least squares estimation. A lag $\delta = 0.12$ s maximizes the relaxation time and minimizes noise amplitude, so we chose it as the time step in numerical simulations.

where τ is the noise relaxation time and a is the noise amplitude³², estimated by analyzing the stochasticity in our data as explained in Fig. 2b. In order to overcome a well known limitation of the OV model, we also include the weighting factor $w(\Delta t)$, which introduces a dependence on time to collision, making the model anticipatory and *collision-free* even under strong nonlinear perturbations:

$$w(\Delta t) = \frac{1}{2} \left[1 + \tanh A \left(-\frac{1}{\Delta t} + B \right) \right], \quad (8)$$

where the parameters A, B are easily derived from first principles³³, effectively switching to deceleration when $\Delta t < 1.5$ s. Finally, the speed adaptation time τ_n is derived by stability considerations (Methods).

Effect of traffic mixture on the capacity

The effect of traffic mixture on the road capacity is evaluated on a finite grid of vehicle concentrations. The capacity-related externalities of micromobility are evident in Fig. 3a-b, where we show a diagram of car flow per lane for different motorcycle shares, which is also in agreement with experimental data. Furthermore, an effective lane capacity of 1600 veh/h agrees with the values reported in the literature for similar infrastructures³⁴. We observe that for a small share of motorcycles, the detrimental effect on car flow is rather negligible and maybe this explains why microvehicles are often not taken into account when studying urban traffic. However, as the motorcycle concentration increases further, the car flow drops drastically in a strongly nonlinear fashion. This is a rather surprising result that contradicts the only known previous numerical study (not validated)³⁵, where a linear reduction in car flow was found. It also appears that the system attains maximum flow at a higher car density than previously reported. Finally, surface plots of space-mean speed as monotonically decreasing function of multispecies concentration are shown, for both species (Fig. 3c-d). Interestingly, for a broad range of traffic mixtures, motorcycle speed becomes insensitive to variations in the car density, a finding which suggests spontaneous separation of flows and merits further, quantitative investigation.

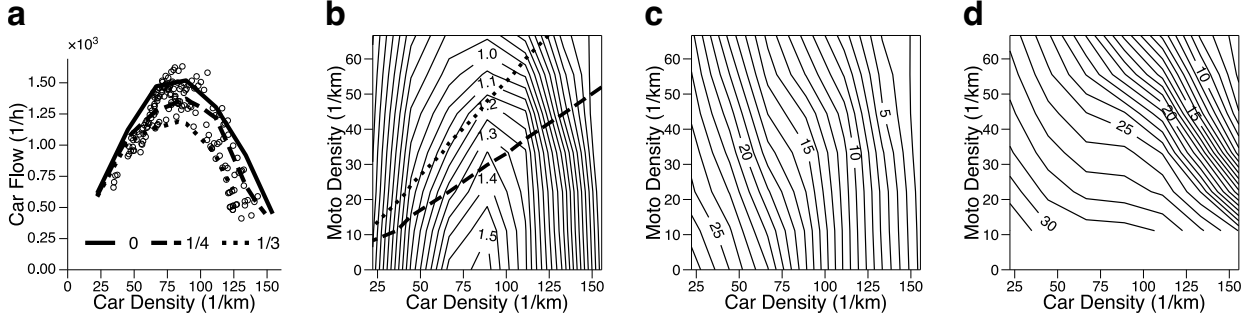


Figure 3: Validation of our nonequilibrium model and numerical simulations under diverse traffic conditions. **(a,b)** Average car flow per lane. The ensemble average flow $\langle Q \rangle$ is calculated as normalized vehicle kilometers traveled (VKT): $\langle Q \rangle = \frac{\langle \text{VKT} \rangle}{(\delta t^* / 3600)(2L / 1000)}$, where δt^* is the effective duration of the simulation and $2L$ is the total lane length. Lines represent simulation results for different motorcycle shares, whereas dots depict quasi-stationary experimental measurements (Supplementary Data 4). **(c)** Average car space-mean speed. **(d)** Average motorcycle space-mean speed. We observe that micovehicles are considerably faster than cars.

Multispecies traffic as DP

While one can argue that the above aggregate traffic variables can be potentially reproduced with a more coarse-grained model, the advantage of our approach is that it also enables the study of nonequilibrium critical phenomena. In this section, we examine the hypothesis that multispecies traffic is an instance of DP, the “most important class of nonequilibrium processes, which display a nontrivial phase transition”³. Phase transitions involve a control parameter and a state variable or order parameter⁹. The control can be for example noise or temperature. In general there is a non-universal critical threshold p_c separating a disordered, subcritical phase from an ordered, supercritical phase and also a universal critical exponent that characterizes the transition. DP in particular is characterized by 3 critical exponents: β , ν_\perp and ν_\parallel . These constants cannot be found analytically, but are known up to an arbitrary numerical accuracy and correspond to 3 variables of state: density, spatial and temporal correlation lengths³. To support the case for DP in multispecies urban traffic, we adopt an *off-lattice formalism*¹⁴ that operates on a moving substrate, rather than the conventional DP on static lattices. This methodological difference should have no effect on the universality of the critical exponents.

Starting with the control parameter, we define the mean view range of all microvehicles at each time step as the temperature T , which is a spatial average:

$$T := \frac{1}{2} \text{nint} \frac{1}{N} \sum_{n=1}^N \alpha_n^+ - \alpha_n^-, \quad (9)$$

where the time dependence is omitted for notational ease and the nearest integer operator is discretizing the view angles at half degree precision. The sum runs over a snapshot of the lane-free population N .

Unlike models of homogeneous systems, the order parameter here must be a relative measure to account for the moving substrate. For each species i , we define the instantaneous order parameter Φ_i :

$$\Phi_i := \frac{1}{N_i} \left\| \sum_{n=1}^{N_i} \frac{\mathbf{v}_n}{V_n(d_{\max})} \right\|, \quad i \in \{\text{car}, \text{moto}\}, \quad (10)$$

where \mathbf{v}_n denotes the velocity vector of agent n and $V_n(d_{\max})$ the respective maximum attainable speed in the simulator. We then compute the difference $\Delta\Phi = \Phi_{\text{moto}} - \Phi_{\text{car}}$ as a measure of percolation. When $\Delta\Phi > 0$, motorcycles are on average faster and may percolate through the cars. However, when $\Delta\Phi < 0$, cars are more efficient because motorcycles are over-maneuvering (substrate is faster).

In order to measure the phase transition, we fix the density and aggregate the simulated data by their temperature T . For each T , the ensemble average $\langle \Delta \Phi \rangle_T$ is computed over all realizations and steps of the random process. Around a critical temperature T_c , that is not universal and depends on the density, $\langle \Delta \Phi \rangle_T \rightarrow 0$ and a nonequilibrium phase transition occurs, as shown in the example of Fig. 4a. For the rest of the analysis, we ignore $\langle \Delta \Phi \rangle_T < 0$ and focus solely on the supercritical case of positive percolation $\langle \Delta \Phi \rangle_T^+$. The inverse quantity $1/\langle \Delta \Phi \rangle_T^+$ would then be analogous to a spatial correlation length that diverges at criticality, where the multispecies system does not have a characteristic scale. This phase transition is governed by a power-law (Fig. 4b):

$$\langle \Delta \Phi \rangle_T^+ \sim |T - T_c|^\nu, \quad T < T_c, \quad (11)$$

where ν is the universal critical exponent. Since DP is a non-integrable process with both path and history dependence, it cannot be solved exactly and no analytical formula exists for the critical threshold³. This implies that equation (11) contains two unknowns: T_c and ν . For each permutation, we fit a distinct power-law by also imposing the optimality condition $T_c = \text{argmin}|\nu - \nu_\perp|$, where ν_\perp is the theoretically expected value of the spatial correlation exponent for 1D DP, as reported in³. Rather than maximizing the goodness of fit, our objective is to minimize the deviation from the theoretical value, thus producing consistent estimates of the critical thresholds.

Our 1D DP hypothesis is unambiguously confirmed with an average $\bar{R}^2 = 0.993$, for the statistically significant density permutations shown in Fig. 4c. These results are presented in greater detail in the appendix (see Supplementary Fig. 2). Accordingly, the normalized critical threshold p_c is clearly non-universal and depends largely on the car density per lane, which indicates the level of traffic congestion. It also appears that the number of microvehicles N has negligible effect on criticality. A lower percolation threshold with higher car density implies that there is a greater chance that even a random arrangement of motorcycles will successfully percolate through the traffic, a finding that aligns with intuition, given the considerable agility of microvehicles.

It is quite remarkable that the complex dynamics of multispecies urban traffic can in fact be reduced to 1 irrational number (Fig. 4b), which is universal and common among all the other porous flows of the same dimensionality, at a macroscopic level. This suggests that, near the thermodynamic limit, heterogeneous, multispecies traffic behaves in the same way as water percolating through a porous medium.

Discussion

In this work we revisit traffic flow theory from the standpoint of complex systems, by first showing that urban traffic is a far-from-equilibrium system and then demonstrating with a nonequilibrium model that multispecies urban traffic has indeed porous characteristics and belongs to the DP universality class. Our result opens a new research avenue for the application of percolation theory to transportation, beyond the scope of existing network models^{36–40}. The nonequilibrium model also accounts for the large scatter observed in recent field data by considering the coexistence and competition between lane-based and lane-free flows. Our open simulation framework can be used to evaluate future scenarios and policies, such as the anticipated increase in lane-free traffic or the performance of connected and automated vehicles in challenging multispecies environments.

It would be interesting and valuable to explore if the universality principles outlined above hold true for other types of heterogeneous crowds, such as a mixed population of pedestrians and e-scooters, or even non-human crowd mixtures. We note that a more comprehensive treatment of the subject should include all 3 exponents that uniquely characterize 1D DP, as well as an investigation of the $\langle \Delta \Phi \rangle_T < 0$ case. Another promising research direction involves the development of a lattice-based, discrete version of our model, which may offer faster computation and be more conducive to theoretical analysis. Finally, we wish to relax the assumption that cars have no lateral dynamics as it is known that lane-changes contribute to traffic congestion and instabilities⁴¹. Therefore, a lane-changing⁴² extension tailored to multispecies traffic is an important next step.

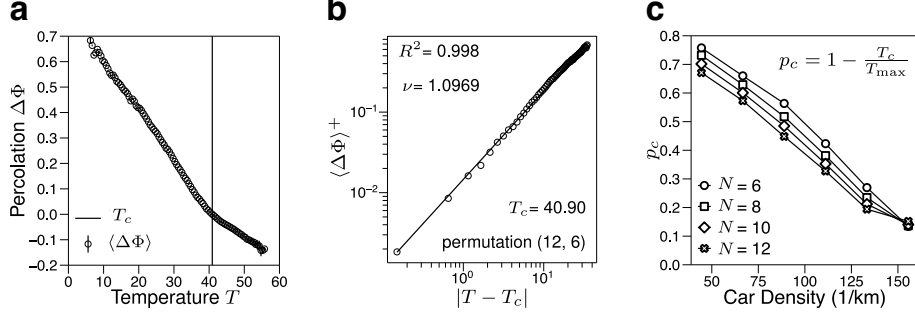


Figure 4: Nonequilibrium phase transition in multispecies traffic. (a) Spatial ensemble averages of the percolation index $\Delta\Phi$ over all simulation runs plotted as a function of T for a specific traffic permutation with 12 cars/lane and $N = 6$ motorcycles. The error bars, which have been obtained by bootstrapping, are barely visible and smaller than the marker size. A sharp discontinuity occurs at the critical temperature T_c despite the relatively small system size with $L = 90$ m. (b) For the same traffic permutation, $\langle\Delta\Phi\rangle_+$ follows an exact power-law having an $R^2 \approx 1$ and a critical exponent $\nu \approx \nu_\perp$. (c) Non-universal normalized percolation thresholds p_c is found by substituting $T_{\max} = 56$ (see Fig. 1c). Each marker corresponds to a statistically significant power-law fit with an average $R^2 = 0.993$ and a standard deviation $\sigma_\nu = 1.4 \times 10^{-5}$.

Methods

Maneuver detection

The real data shown in Fig. 1c are produced by our maneuver detection algorithm. This method requires 3 inputs: vehicle positions (x, y) , vehicle azimuth θ_{veh} and road azimuth θ_0 . Then, we proceed to define the instantaneous relative angle $\theta = \theta_{\text{veh}} - \theta_0$ and the curvature $\kappa = \frac{d\theta}{dr}$ with respect to the arch traveled r . Trajectory points with $\kappa = 0$ are essentially inflection points, where the curvature changes sign or, in terms of driving/riding, a steering event occurs. Steering events occur regularly in cruising but become sparse during maneuvering. By detecting such sparsity, we can reliably detect and characterize any maneuver.

Leader identification

Unlike constant-speed simulations, such as the ones produced with Vicsek's model, leader identification is relevant in dynamic traffic models. More specifically, leading agents in 2D are determined by a heuristic known as the overlap criterion, which is explained in²⁰ and references therein. This is simply a stripe, as shown in Fig. 1a, of exactly the same width as the

ego vehicle and infinite length. Taking into account the size of our simulator and the fact that periodic boundary conditions are in place, we set the stripe length equal to the horizon distance $d_{\max} = 40$ m. Unfortunately, this criterion neglects lateral frictions that interrupt the pure follow-the-leader behavior, a phenomenon that has been empirically observed in the pNEUMA experiment. Consequently, we enlarge the stripe width by a factor $f = 1.5$ that permits the detection of laterally adjacent agents. Our adapted overlap criterion introduces asymmetric effects as it depends on vehicle size, which varies considerably in traffic mixtures. Including lateral friction prevents unrealistic crashes between microvehicles and also generates realistic nonlinear perturbations in the car platoons, which have an impact on the capacity.

Stability considerations

Consider N vehicles from the same or different species. The equilibrium spacing s_n^* of each vehicle n is found by solving for the equilibrium velocity v^* :

$$\sum_{n=1}^N s_n^* = \sum_{n=1}^N V_n^{-1}(v^*) = 2L - \sum_{n=1}^N \ell_n, \quad (12)$$

subject to $0 < v^* < \inf_n v_n^0$. $2L$ is the total road length, including both lanes, and ℓ_n is the vehicle length. Then from the strict stability criterion for heterogeneous traffic which is known as combination stability⁴³, we obtain the implicit speed adaptation time τ_n for each agent n :

$$\tau_n = \max \left\{ \left[1 + \cos \frac{2\pi}{N} \right] V'_n(s_n^*), \lambda_n \right\}^{-1}, \quad (13)$$

subject to $s_n^* > s_n^0$. The term in square brackets approaches 2 as $N \rightarrow \infty$ resulting in more precise stability bounds for finite rings⁴⁴. Notice that the stochastic component of the model does not impact the stability because it only captures imperfections in the optimal velocity function as opposed to driver control or acceleration errors^{45,46}.

Numerical scheme

For the numerical computation of Δt we use a Newton-Raphson iteration with tolerance of 10^{-4} s. The solution to the stochastic differential equations follows the Euler-Maruyama integration scheme^{32,46} with a time step $\delta = 0.12$ s:

$$\begin{cases} \varepsilon_n(t + \delta) = (1 - \delta\tau^{-1})\varepsilon_n(t) + a\sqrt{\delta}\eta_n, \\ v_n(t + \delta) = v_n(t) + \delta \frac{w[V_n + \varepsilon_n(t + \delta)] - v_n(t)}{\tau_n}, \\ x_n(t + \delta) = x_n(t) + \delta v_n(t + \delta), \end{cases} \quad (14)$$

where each independent $\eta_n \stackrel{iid}{\sim} \mathcal{N}(0, 1)$. In terms of operational navigation, agents steer smoothly with a global relaxation time $\tau = 0.6$ s, a value within the range reported in several other studies^{18,20,28}:

$$\alpha_n(t + \delta) = \alpha_n(t) + \delta \frac{\alpha_n^{\text{des}}(t) - \alpha_n(t)}{\tau}. \quad (15)$$

Data availability

We analyzed extensive field data, which is available at <https://open-traffic.epfl.ch>. The data sample used in this paper was collected on October 24, 2018, between 9:30 and 10:00, using drone D8. The sample was preprocessed using anomaly detection and data smoothing techniques specifically designed for traffic monitoring with a swarm of drones⁴⁷.

Code availability

The custom simulation software for replicating the methods and results outlined in the paper, along with the corresponding documentation, is publicly available on GitHub at: <https://github.com/EPFL-ENAC/LUTS-pneuma-simulator>.

References

1. Nair, R., Mahmassani, H. S. & Miller-Hooks, E. A porous flow approach to modeling heterogeneous traffic in disordered systems. *Transportation Research Part B: Methodological* **45**, 1331–1345 (Nov. 2011).
2. Stauffer, D. & Aharony, A. *Introduction to percolation theory* 2nd ed. en (Taylor & Francis, London, England, July 1994).
3. Hinrichsen, H. Non-equilibrium critical phenomena and phase transitions into absorbing states. *Advances in Physics* **49**, 815–958 (Nov. 2000).
4. O’Hern, S. & Estegfaeller, N. A scientometric review of powered micromobility. *Sustainability* **12**, 9505 (2020).
5. Mason, A. D. & Woods, A. W. Car-following model of multispecies systems of road traffic. *Physical Review E* **55**, 2203–2214 (Mar. 1997).
6. Barmounakis, E. & Geroliminis, N. On the new era of urban traffic monitoring with massive drone data: The pNEUMA large-scale field experiment. *Transportation Research Part C: Emerging Technologies* **111**, 50–71 (Feb. 2020).
7. Thurner, S., Klimek, P. & Hanel, R. *Introduction to the Theory of Complex Systems* (Oxford University Press, Nov. 2018).
8. Bak, P., Tang, C. & Wiesenfeld, K. Self-organized criticality: An explanation of the 1/f noise. *Physical review letters* **59**, 381 (1987).
9. Stanley, H. *Introduction to Phase Transitions and Critical Phenomena* (Oxford University Press, 1987).

10. Lighthill, M. J. & Whitham, G. B. On kinematic waves II. A theory of traffic flow on long crowded roads. *Proceedings of the royal society of london. series a. mathematical and physical sciences* **229**, 317–345 (1955).
11. Richards, P. I. Shock waves on the highway. *Operations research* **4**, 42–51 (1956).
12. Benzoni-Gavage, S. & Colombo, R. M. An n -populations model for traffic flow. *European Journal of Applied Mathematics* **14**, 587–612 (2003).
13. Zhang, H. A theory of nonequilibrium traffic flow. *Transportation Research Part B: Methodological* **32**, 485–498 (Sept. 1998).
14. Vicsek, T., Czirók, A., Ben-Jacob, E., Cohen, I. & Shochet, O. Novel type of phase transition in a system of self-driven particles. *Physical review letters* **75**, 1226 (1995).
15. Bain, N. & Bartolo, D. Critical mingling and universal correlations in model binary active liquids. *Nature Communications* **8** (June 2017).
16. Schmiedeberg, M. Far from the equilibrium crowd. *Nature Physics* **19**, 1078–1079 (July 2023).
17. Ondřej, J., Pettré, J., Olivier, A.-H. & Donikian, S. A synthetic-vision based steering approach for crowd simulation. *ACM Transactions on Graphics (TOG)* **29**, 1–9 (2010).
18. Moussaïd, M., Helbing, D. & Theraulaz, G. How simple rules determine pedestrian behavior and crowd disasters. *Proceedings of the National Academy of Sciences* **108**, 6884–6888 (Apr. 2011).
19. Karamouzas, I., Skinner, B. & Guy, S. J. Universal power law governing pedestrian interactions. *Physical review letters* **113**, 238701 (2014).
20. Xu, Q., Chraïbi, M. & Seyfried, A. Anticipation in a velocity-based model for pedestrian dynamics. *Transportation Research Part C: Emerging Technologies* **133**, 103464 (Dec. 2021).
21. Zheng, X. & Palfy-Muhoray, P. Distance of closest approach of two arbitrary hard ellipses in two dimensions. *Physical Review E* **75** (June 2007).
22. Stumpf, M. P. & Porter, M. A. Critical truths about power laws. *Science* **335**, 665–666 (2012).
23. Gigerenzer, G. Why heuristics work. *Perspectives on psychological science* **3**, 20–29 (2008).
24. Corominas-Murtra, B., Hanel, R. & Thurner, S. Understanding scaling through history-dependent processes with collapsing sample space. *Proceedings of the National Academy of Sciences* **112**, 5348–5353 (Apr. 2015).
25. Corominas-Murtra, B., Hanel, R. & Thurner, S. Sample space reducing cascading processes produce the full spectrum of scaling exponents. *Scientific Reports* **7** (Sept. 2017).
26. Bridson, R. *Fast Poisson disk sampling in arbitrary dimensions* in *ACM SIGGRAPH 2007 sketches* (ACM, Aug. 2007).
27. Koenker, R. & Hallock, K. F. Quantile regression. *Journal of economic perspectives* **15**, 143–156 (2001).
28. Guo, N. *et al.* Bicycle flow dynamics on wide roads: Experiments and simulation. *Transportation Research Part C: Emerging Technologies* **125**, 103012 (Apr. 2021).
29. Bando, M., Hasebe, K., Nakayama, A., Shibata, A. & Sugiyama, Y. Dynamical model of traffic congestion and numerical simulation. *Physical Review E* **51**, 1035–1042 (Feb. 1995).
30. Newell, G. F. Nonlinear effects in the dynamics of car following. *Operations research* **9**, 209–229 (1961).
31. Daganzo, C. F. In Memoriam: Gordon F. Newell, 1925–2001. *Transportation Science* **35**, iii–v (2001).
32. Tordeux, A. & Schadschneider, A. White and relaxed noises in optimal velocity models for pedestrian flow with stop-and-go waves. *Journal of Physics A: Mathematical and Theoretical* **49**, 185101 (Apr. 2016).

33. Mammar, S., Mammar, S. & Haj-Salem, H. A modified optimal velocity model for vehicle following. *IFAC Proceedings Volumes* **38**, 120–125 (2005).
34. Wu, X., Liu, H. X. & Geroliminis, N. An empirical analysis on the arterial fundamental diagram. *Transportation Research Part B: Methodological* **45**, 255–266 (Jan. 2011).
35. Lan, L. W., Chiou, Y.-C., Lin, Z.-S. & Hsu, C.-C. Cellular automaton simulations for mixed traffic with erratic motorcycles’ behaviours. *Physica A: Statistical Mechanics and its Applications* **389**, 2077–2089 (May 2010).
36. Li, D. *et al.* Percolation transition in dynamical traffic network with evolving critical bottlenecks. *Proceedings of the National Academy of Sciences* **112**, 669–672 (Dec. 2014).
37. Olmos, L. E., Çolak, S., Shafiei, S., Saberi, M. & González, M. C. Macroscopic dynamics and the collapse of urban traffic. *Proceedings of the National Academy of Sciences* **115**, 12654–12661 (Dec. 2018).
38. Saberi, M. *et al.* A simple contagion process describes spreading of traffic jams in urban networks. *Nature Communications* **11** (Apr. 2020).
39. Zeng, G. *et al.* Multiple metastable network states in urban traffic. *Proceedings of the National Academy of Sciences* **117**, 17528–17534 (July 2020).
40. Ambühl, L., Menendez, M. & González, M. C. Understanding congestion propagation by combining percolation theory with the macroscopic fundamental diagram. *Communications Physics* **6** (Feb. 2023).
41. Laval, J. A. & Daganzo, C. F. Lane-changing in traffic streams. *Transportation Research Part B: Methodological* **40**, 251–264 (Mar. 2006).
42. Kesting, A., Treiber, M. & Helbing, D. General lane-changing model MOBIL for car-following models. *Transportation Research Record* **1999**, 86–94 (2007).
43. Yang, D., Jin, P. J., Pu, Y. & Ran, B. Stability analysis of the mixed traffic flow of cars and trucks using heterogeneous optimal velocity car-following model. *Physica A: Statistical Mechanics and its Applications* **395**, 371–383 (2014).
44. Huijberts, H. J. C. Improved stability bound for steady-state flow in a car-following model of road traffic on a circular route. *Physical Review E* **65** (Apr. 2002).
45. Laval, J. A. & Leclercq, L. A mechanism to describe the formation and propagation of stop-and-go waves in congested freeway traffic. *Philosophical Transactions of the Royal Society A: Mathematical, Physical and Engineering Sciences* **368**, 4519–4541 (Oct. 2010).
46. Ngoduy, D., Lee, S., Treiber, M., Keyvan-Ekbatani, M. & Vu, H. Langevin method for a continuous stochastic car-following model and its stability conditions. *Transportation Research Part C: Emerging Technologies* **105**, 599–610 (Aug. 2019).
47. Kim, S., Anagnostopoulos, G., Barmounakis, E. & Geroliminis, N. Visual extensions and anomaly detection in the pNEUMA experiment with a swarm of drones. *Transportation Research Part C: Emerging Technologies* **147**, 103966 (Feb. 2023).

Acknowledgements

Our paper was partially funded by the Swiss National Science Foundation (SNSF) grant 200021_188590 “pNEUMA: On the new era of urban traffic models with massive empirical data from aerial footage”.

Author contributions

GA and NG designed the research. GA performed the numerical simulations. GA and NG developed the theory, discussed the results and wrote the paper.